ISSN 1674-1056
http://cpb.iphy.ac.cn
http://iopscience.iop.org/cpb
中国物理 B
Chinese Physics
中国物理
Chinese Physics B

Calculation of the infrared frequency and the damping constant (full width at half maximum) for metal organic frameworks

M Kurt, H Yurtseven, A Kurt, S Aksoy

Citation: Chin. Phys. B . 2019, 28(6): 066401. **doi:** 10.1088/1674-1056/28/6/066401
Journal homepage: http://cpb.iphy.ac.cn; http://iopscience.iop.org/cpb

What follows is a list of articles you may be interested in

Transport properties of mixing conduction in CaF_2 nanocrystals under high pressure

Ting-Jing Hu(胡廷静), Xiao-Yan Cui(崔晓岩), Jing-Shu Wang(王婧姝), Jun-Kai Zhang(张俊凯), Xue-Fei Li(李雪飞), Jing-Hai Yang(杨景海), Chun-Xiao Gao(高春晓)

Chin. Phys. B . 2018, 27(1): 016401. **doi:** 10.1088/1674-1056/27/1/016401

High pressure electrical transport behavior in SrF_2 nanoplates

Xiao-Yan Cui(崔晓岩), Ting-Jing Hu(胡廷静), Jing-Shu Wang(王婧姝), Jun-Kai Zhang(张俊凯), Xue-Fei Li(李雪飞), Jing-Hai Yang(杨景海), Chun-Xiao Gao(高春晓)

Chin. Phys. B . 2017, 26(4): 046401. **doi:** 10.1088/1674-1056/26/4/046401

Carrier behavior of HgTe under high pressure revealed by Hall effect measurement

Hu Ting-Jing, Cui Xiao-Yan, Li Xue-Fei, Wang Jing-Shu, Lü Xiu-Mei, Wang Ling-Sheng, Yang Jing-Hai, Gao Chun-Xiao

Chin. Phys. B . 2015, 24(11):116401. **doi:** 10.1088/1674-1056/24/11/116401

Phase behaviors of binary mixtures composed of banana-shaped and calamitic mesogens

M. Cvetinov, D. Ž. Obadović, M. Stojanović, A. Vajda, K. Fodor-Csorba, N. Eber, I. Ristić

Chin. Phys. B . 2014, 23(9): 096402. **doi:** 10.1088/1674-1056/23/9/096402

Characteristics of phase transitions via intervention in random networks

Jia Xiao, Hong Jin-Song, Yang Hong-Chun, Yang Chun, Shi Xiao-Hong, Hu Jian-Quan

Chin. Phys. B . 2014, 23(7): 076401. **doi:** 10.1088/1674-1056/23/7/076401

Calculation of the infrared frequency and the damping constant (full width at half maximum) for metal organic frameworks

M Kurt[1,†], H Yurtseven[2], A Kurt[3], and S Aksoy[1]

[1] *Department of Physics, Çanakkale* 18 *Mart University*, 17100 *Çanakkale, Turkey*
[2] *Department of Physics, Middle East Technical University*, 06531 *Ankara, Turkey*
[3] *Lapseki İÇDAŞ ÇİB MTAL High School*, 17100 *Çanakkale, Turkey*

(Received 28 January 2019; revised manuscript received 10 April 2019; published online 29 May 2019)

The $\rho(NH_2)$ infrared (IR) frequencies and the corresponding full width at half maximum (FWHM) values for $(CH_3)_2NH_2Fe^{III}M^{II}(HCOO)_6$ (DMFeM, M =Ni, Zn, Cu, Fe, and Mg) are analyzed at various temperatures by using the experimental data from the literature. For the analysis of the IR frequencies of the $\rho(NH_2)$ mode which is associated with the structural phase transitions in those metal structures, the temperature dependence of the mode frequency is assumed as an order parameter and the IR frequencies are calculated by using the molecular field theory. Also, the temperature dependence of the IR frequencies and of the damping constant as calculated from the models of pseudospin (dynamic disorder of dimethylammonium (DMA^+) cations)–phonon coupling (PS) and of the energy fluctuation (EF), is fitted to the observed data for the wavenumber and FWHM of the $\rho(NH_2)$ IR mode of the niccolites studied here. We find that the observed behavior of the IR frequencies and the FWHM of this mode can be described adequately by the models studied for the crystalline structures of interest. This method of calculating the frequencies (IR and Raman) and FWHM of modes which are responsible for the phase transitions can also be applied to some other metal organic frameworks.

Keywords: infrared (IR) frequency, full width at half maximum (FWHM), phase transitions, $\rho(NH_2)$ mode, niccolites

PACS: 64.10.+h, 64.60.–I, 64.70.–p **DOI:** 10.1088/1674-1056/28/6/066401

1. Introduction

A large number of studies have been devoted to the metal-organic frameworks (MOFs) since they have many applications as catalysts, chemical tensors, and luminescent materials.[1–3] Organic-based MOFs have attracted a lot of attention in recent years mainly due to their multiferroic properties.[4–11]

Among the MOFs, novel niccolites with the formula $(CH_3)_2NH_2Fe^{III}M^{II}(HCOO)_6$ (M^{II} =Ni, Zn, Cu, Fe, and Mg), shortly, DMFeNi, DMFeZn, DMFeCu,[12] DMFeFe, and DMFeMg,[13] have been studied to investigate their structures, thermal, magnetic, and vibrational (Raman and infrared (IR)) properties. DMFeNi and DMFeZn crystallize in the trigonal structure (space group $P\bar{3}1c$) while DMFeCu crystallizes in the monoclinic structure (space group $C2/c$).[12] DMFeFe crystallizes in the niccolite type structure (space group $P\bar{3}1c$) with the disordered dimethylammonium (DMA^+) cations in the cages of the network[14] and it undergoes antiferroelectric phase (space group $R\bar{3}c$) at 155 K,[15] as also pointed out previously.[13] DMFeFe shows a sharp heat anomaly at 155.2 K upon warming and 151.8 K upon cooling, characteristic for a first order phase transition, whereas DMFeMg does not undergo any phase transition down to 125 K.[13]

Regarding vibrational properties of these niccolite compounds, the observed Raman and IR bands have been assigned to internal vibrations and librations of the DMA^+ and formate ions as well as translational motions of these ions and metal cations for DMFeNi, DMFeZn, DMFeCu,[12] DMFeFe, and DMFeMg.[13] In the case of DMA^+, the internal modes can be stretching $\upsilon(NH_2)$, scissoring $\delta(NH_2)$, rocking $\rho(NH_2)$, wagging $\omega(NH_2)$, and torsion or twisting $\tau(NH_2)$ modes of the NH_2 group with the internal modes of the CNC and CH_3 groups.[12]

In this study, we analyze the IR frequencies of the internal $\rho(NH_2)$ mode by using the observed data for the compounds of DMFeNi, DMFeZn, and DMFeCu[12] and, DMFeFe and DMFeMg[13] below and above the critical temperature T_c for their phase transitions. Among these niccolites, DMFeFe exhibits structural phase transition. The temperature dependence of the IR frequency associated with the order parameter is calculated by the molecular field theory. Also, the damping constant (linewidth) of this mode is calculated through the pseudospin–phonon coupling (PS) and the energy fluctuation (EF) models for these niccolite compounds by using the observed full width at half maximum (FWHM) data.[12,13]

Below, in Section 2, we give our calculations and results. Discussion of our results is given in Section 3. We give our conclusions in Section 4.

†Corresponding author. E-mail: mkurt@comu.edu.tr

2. Calculations and results

The temperature dependence of the order parameter and the damping constant can be derived from the pseudospin–phonon interaction energy. An Ising pseudospin–phonon coupled model has been developed by Yamada *et al.*[16] by considering interaction between pseudospin and one phonon in molecular crystals. This model of Yamada *et al.* has been modified in terms of the interactions between pseudospin and more than one phonon by Matsushita.[17] He derived expressions for the frequency and the damping constant of phonons from his Hamiltonian and predicted mainly the temperature dependence of the optic phonons in ammonium halides (NH_4Br and NH_4Cl).[17] According to the model of Yamada *et al.*,[16] Hamiltonian for the Ising pseudospin–phonon interaction is given by

$$H = \frac{1}{2}\sum (p_{\boldsymbol{k}s}p^*_{\boldsymbol{k}s} + \omega^2_{\boldsymbol{k}s}q_{\boldsymbol{k}s}q^*_{\boldsymbol{k}s}) - \frac{1}{2}\sum_{ij} J_{ij}\sigma_i\sigma_j - \sum_{\boldsymbol{k}s}\sum_i \frac{\omega_{\boldsymbol{k}s}}{\sqrt{N}} g_{\boldsymbol{k}s}q_{\boldsymbol{k}s}\sigma_i \mathrm{e}^{\mathrm{i}\boldsymbol{k}\cdot\boldsymbol{r}_i}. \tag{1}$$

In Eq. (1), $q_{\boldsymbol{k}s}$ is the phonon coordinate for the s mode ($\boldsymbol{k}$ is the wave vector), $\omega_{\boldsymbol{k}s}$ is the characteristic frequency, and $p_{\boldsymbol{k}s}$ is the momentum of the phonon. The first term in Eq. (1) defines phonon energy. In the second term of Eq. (1), σ is the spin variable with the nearest neighbor interaction parameter (J_{ij}) in an Ising model. The third term defines the interaction between pseudospin (σ_i) and phonon ($q_{\boldsymbol{k}s}$) with the interaction parameter $g_{\boldsymbol{k}s}$. This Hamiltonian defines the interaction between pseudospin and one phonon only. As stated above, the Hamiltonian of Yamada *et al.* (Eq. (1)) has been extended by Matsushita, considering the interaction between pseudospin and phonons, and from his Hamiltonian, he derived the expressions for the frequency and damping constant of phonons.[17] According to his derivations, the phonon frequency is given by

$$\omega^2 = \bar{\omega}^2_0(\boldsymbol{k}\nu,\omega) + K_1(\boldsymbol{k},\boldsymbol{q}=0,\nu\nu')\langle(\sigma(\boldsymbol{q}=0))\rangle + \sum_{\boldsymbol{q}} K_2(\boldsymbol{k},\boldsymbol{q},-\boldsymbol{q},\nu\nu')\langle|\sigma(\boldsymbol{q})|^2\rangle + \mathrm{Re}\sum_{sp}(\boldsymbol{k}\nu,\omega). \tag{2}$$

In Eq. (2), the first term defines anharmonic phonon energy. In the second term, $\langle\sigma(\boldsymbol{q}=0)\rangle$ is the order parameter and the parameter K_1 is the coupling of the two phonons ($\boldsymbol{k}\nu$ and $\boldsymbol{k}\nu'$) with the wavevector $\boldsymbol{q}=0$, whereas the parameter K_2 is the coupling of the two phonons ($\boldsymbol{k}\nu$ and $\boldsymbol{k}\nu'$) and two pseudospins with the wave vectors $\boldsymbol{q}$ and $-\boldsymbol{q}$. $|\sigma(\boldsymbol{q})|^2$ represents the spin–spin correlation function. Equation (2) gives that the phonon frequency is essentially the real part of the pseudospin–phonon (sp) interaction energy. Similarly, from the derivation of the damping constant of phonons by Matsushita[17] in terms of the dynamic scattering function, the damping constant is defined as the imaginary part of the pseudospin–phonon interaction energy which is given by

$$\mathrm{Im}\sum_{sp}(\boldsymbol{k}\nu,\omega) = 2\omega\Gamma_{sp}(\boldsymbol{k}\nu,\omega). \tag{3}$$

Regarding the metal-organic frameworks (MOFs) as studied here, the Ising pseudospin (Eq. (1)) corresponds to the DMA^+ cations due to their re-orientational motions at low temperatures (below T_c). The ordering of DMA^+ cations is associated with the distortion of the metal-organic frameworks. Spectroscopically, changes in frequencies and bandwidth are observed for phonon which involve motions so that one can assume the pseudospin–phonon coupling with a positive or negative coupling constant as also indicated previously.[13] In Eq. (1), the second term describes the interaction between nearest-neighbor DMA^+ cations as pseudospins, and the third term is due to the interaction between DMA^+ cation and the distorted metal organic framework as the pseudospin–phonon coupling in the Ising pseudospin–phonon coupled model of Yamada *et al.* In the case of Matsushita's model which considers more than one pseudospin and phonon, frequency and the damping constant (bandwidth) can be described by Eqs. (2) and (3), respectively, for the metal-organic frameworks (MOFs). The second term in Eq. (2) describes the coupling between two phonons and the DMA^+ cation (pseudospin), with the coupling constant K_1, the third term is due to the coupling between two phonons and two DMA^+ cations (pseudospins) with the real part of the DMA^+ cation–phonon interaction energy. As stated above, the imaginary part of the pseudospin–phonon interaction energy describes the damping constant (bandwidth) of those phonons interacting with the DMA^+ cations, which are involved in the mechanism of the phase transitions in MOFs.

Since the critical behavior of the damping constant Γ_{sp} is governed by the dynamic scattering function in the Matsushita's expression,[17] which can be integrated over all $\boldsymbol{q}$ in the Brillouin zone, temperature dependence of the damping constant is obtained near T_c as

$$\Gamma_{sp} = \Gamma_0 + A\,(1-S^2)\,\ln\left(\frac{T_c}{T - T_c(1-S^2)}\right), \tag{4}$$

where S is the order parameter as given in an earlier study.[18] Damping constant is also obtained using another approach[19] for the pseudospin–phonon interaction as

$$\Gamma_{sp} = \Gamma'_0 + A'\left[\frac{T(1-S^2)}{T - T_c(1-S^2)}\right]^{1/2}. \tag{5}$$

In Eqs. (4) and (5), Γ_0 (Γ'_0) is the background damping constant (linewidth) and A (A') represents the amplitude. The

expressions for the temperature dependence of the damping constant Γ_{sp}, namely, from the pseudospin–phonon coupling model (Eq. (4)) and the energy-fluctuation model (Eq. (5)), have been obtained and applied to potassium dihydrogen phosphat (KDP) type crystals previously.[20]

Matsushita[17] also derived an expression by using the molecular field theory[21] for the temperature dependence of the order parameter $\langle\sigma(q_0)\rangle$ which we denote by S as given by

$$S = [3(1-T/T_c)]^{1/2}, \qquad 0 < (T_c - T) < T, \tag{6a}$$

$$= 1 - 2\exp(-2T_c/T), \qquad T \ll T_c, \tag{6b}$$

$$= 0, \qquad T > T_c. \tag{6c}$$

We have given these expressions of the phonon frequency and damping constant (Eqs. (4) and (5)) and the order parameter (Eqs. (6a)–(6c)) to some extended from the Madsushita's theory as applied to the λ phase transitions in ammonium halides in our previous study.[22]

This behavior of the order parameter can be associated with the temperature dependence of the frequencies for various Raman and IR modes in metal organic frameworks, in particular for DMFeM (M =Ni, Zn, Cu, Fe, and Mg) structures. Thus, by assuming the Raman and/or IR frequency of modes associated with the mechanism of the order–disorder transitions in those heterometallic MOFs as an order parameter S, Raman and IR frequencies can be calculated from the molecular field theory (Eqs. (6a)–(6c)). By considering the temperature dependence of the frequency υ (Raman or IR) as

$$\upsilon/\upsilon_{max} = a_o + a_1 T + a_2 T^2, \tag{7}$$

where a_0, a_1, and a_2 are constants and υ_{max} denotes the maximum value of the frequency, frequency can be related to the order parameter S according to the quadratic relation

$$S = a + b(\nu/\nu_{max}) + c(\nu/\nu_{max})^2 \tag{8}$$

with the constants a, b, and c.

The damping constant (linewidth) of those Raman and IR modes associated with the freezing-in of molecular motions of DMA^+ cations can also be calculated at various temperatures for heterometallic compounds studied by using their frequencies (Raman or IR) as an order parameter. For this calculation, the two models are chosen, namely, the pseudospin–phonon coupling model[18] and the energy fluctuation model,[19] both depending on the order parameter according to Eqs. (4) and (5), respectively, as given above.

For heterometallic crystals due to the freezing-in of motions of the DMA^+ cations with the critical temperature T_c below which reorientational motions of DMA^+ are frozen, those two models (PS and EF) are employed to calculate the temperature dependence of the damping constant (linewidth) in these structures.

In this study, we have calculated the IR frequencies of the $\rho(NH_2)$ mode by analyzing the observed data[12] (Eq. (7)), and the order parameter (Eqs. (6a)–(6c)) by means of Eq. (8) for DMFeM (M =Ni, Zn, Cu, Fe, and Mg). Table 1 gives the values of the parameters $a_0(=1)$, a_1, and a_2 determined (Eq. (7)) for the $\rho(NH_2)$ mode of those niccolite structures. Above T_c, we give values of those parameters (a_0, a_1, and a_2) according to Eq. (7) in Table 2.

Table 1. Values of the coefficients $a_0 = 1$, a_1, a_2 (Eq. (7)), a, b, and c (Eq. (8)) below T_c ($T < T_c$) within the temperature intervals for the niccolite compounds indicated. Values of the critical temperature T_c and the maximum frequency υ_{max} of the $\rho(NH_2)$ IR mode are also given.

MOFs	T_c/K	ν_{max}	$-a_1\times10^{-5}/K^{-1}$	$a_2\times10^{-8}/K^{-2}$	$-a$	b	$-c$	Temperature interval/K
DMFeNi	160	867.4	3.85	−17.9	3185.18	6375.42	3189.24	$4 < T < 160$
DMFeZn	220	869.4	7.85	3.37	1960.99	3934.09	1972.11	$4 < T < 220$
DMFeCu	100	909.8	4.62	−0.37	4517.49	9036.44	4517.95	$4 < T < 100$
DMFeMg	151.8	864.4	3.83	1.45	14963.9	29956.72	14991.82	$4.6 < T < 140.8$
DMFeFe	151.8	858.3	2.61	2.89	62583.93	125111.12	62526.21	$40.1 < T < 140.4$

Table 2. Values of the coefficients a_0, a_1, a_2 (Eq. 7) above T_c ($T > T_c$) within the temperature intervals for the niccolite compounds indicated. Values of the critical temperature (T_c) and the maximum frequency (ν_{max}) of the $\rho(NH_2)$ IR mode are also given.

MOFs	T_c/K	ν_{max}	a_0	$-a_1\times10^{-5}/K^{-1}$	$a_2\times10^{-8}/K^{-2}$	Temperature interval/K
DMFeNi	160	867.4	0.992	0.33	−8.61	$160 < T < 300$
DMFeZn	220	869.4	0.998	6.46	3.35	$160 < T < 300$
DMFeCu	100	909.8	0.998	3.62	−2.33	$100 < T < 300$
DMFeMg	151.8	864.4	1.007	10.70	14.96	$152 < T < 300$
DMFeFe	151.8	858.3	1.011	8.96	10.43	$152 < T < 300$

By calculating the order parameter S (Eqs. (6a) and (6b)) below T_c and fitting S to the observed frequencies (ν data)[12,13] according to Eq. (8) with the parameters a, b, and c (as listed in Table 1), we are able to obtain the IR frequencies of the

$\rho(NH_2)$ mode ($T < T_c$) for DMFeM (M = Ni, Zn, Cu, Fe, and Mg). We plot variation of the wavenumber of the $\rho(NH_2)$ mode with temperature for DMFeNi and DMFeZn (Fig. 1), DMFeCu (Fig. 2), and frequency of the $\rho(NH_2)$ mode as a function of temperature for DMFeFe and DMFeMg (Fig. 3). In these figures, observed data for DMFeM (M = Ni, Zn, and Cu)[12] and for DMFeM (M = Fe, Mg)[13] are also given. Solid lines represent our fits below T_c (Eqs. (7) and (8)) and above T_c (Eq. (7)). We then calculate the damping constant as a function of temperature according to Eqs. (4) and (5), which are fitted to the observed FWHM data[12,13] for the $\rho(NH_2)$ IR mode with the values of Γ_0 (Γ_0') and A (A') as determined (as listed in Table 3).

Table 3. Values of the background damping constant (linewidth) Γ_0 (Γ_0') and the amplitude A (A') according to the pseudospin–phonon (PS) model (Eq. 4) and the energy-fluctuation (EF) model (Eq. 5) within the temperature intervals for the niccolite compounds indicated. The T_c values are also given here.

MOFs	T_c/K	PS model		EF model		Temperature interval/K
		Γ_0/cm^{-1}	A/cm^{-1}	Γ_0'/cm^{-1}	$-A'$/cm^{-1}	
DMFeNi	160	30.56	−6.91	23.46	0.54	$4 < T < 160$
DMFeZn	220	25.70	−4.50	20.82	0.29	$4 < T < 220$
DMFeCu	100	6.08	9.61	–	–	–
DMFeMg	151.8	8.54	1.74	10.36	0.13	$4.6 < T < 140.8$
DMFeFe	151.8	5.06	1.05	6.05	0.09	$40.8 < T < 100.9$
		−14.4	11.71	−5.10	1.19	$120.6 < T < 140.4$

Note that we use Eq. (6a) in Eqs. (4) and (5) for the DMFeNi and DMFeZn, and the results are shown in Figs. 4 and 5, respectively. For the calculation of the damping constant of DMFeCu, we use Eq. (6b) in Eq. (4), the calculated results are shown in Fig. 6. We do not gain any good fit by using Eqs. (6a) or (6b) in Eq. (5) for DMFeCu, so we exclude the damping constant predicted from the energy fluctuation model for DMFeCu. Finally, we calculate the damping constant of the $\rho(NH_2)$ IR mode for DMFeFe and DMFeMg according to the PS (Eq. (4)) and EF (Eq. (5)) models. By using Eq. (6a) in Eqs. (4) and (5), which are fitted to the experimental FWHM data,[13] damping constant (Γ_{sp}) is obtained as a function of temperature, as plotted in Fig. 7 (PS model) and Fig. 8 (EF model).

3. Discussion

The IR frequencies of the $\rho(NH_2)$ internal mode are calculated at various temperatures for niccolate compounds of DMFeM (M = Ni, Zn, Cu, Fe, and Mg) as plotted in Figs. 1–3, from the molecular field theory (Eqs. (6a)–(6c)) by fitting the order parameter S (frequency) to the observed data[12,13] through Eq. (8) below T_c with the fitted parameters (Table 1). This fit is performed by Eq. (7) since we assume that the order parameter is zero ($S = 0$) above T_c with the fitted parameters (Table 2) in those niccolate structures.

Our fits are reasonable in both regions (below and above T_c) for those crystals which indicates, in particular below T_c, that the IR frequency of the $\rho(NH_2)$ internal mode can be associated with the order parameter S according to the molecular field theory (Eqs. (6a)–(6c)). The temperature below which DMA^+ cations do not exhibit jumps between equivalent sites is more apparent for DMFeNi ($T_c \approx 160$ K) as compared to DMFeZn ($T_c \approx 220$ K), and DMFeCu ($T_c \approx 100$ K). It has been pointed out that DMFeCu exhibits short range ordering of DMA^+ cations at low temperatures, whereas DMFeNi and DMFeZn show evolution of dynamic disorder into static disorder.[12] This ordering due to freezing-in of molecular motions of DMA^+ cations as stated above, can be associated with temperature dependence of the wavenumber for the $\rho(NH_2)$ internal mode. Due to the internal vibrations of the DMA^+ and formate ions in those heterometalic compounds (DMFeNi, DMFeZn, and DMFeCu), the $\rho(NH_2)$ mode among the six internal modes has been observed in all trigonal compounds (DMFeNi and DMFeZn) at room temperature, whereas for the monoclinic DMFeCu, it has appeared at low temperatures with higher wavenumbers.[12] Existence of this mode at higher frequencies in DMFeCu (Fig. 2) indicates that the hydrogen bonds are stronger in the monoclinic structures as compared to the trigonal niccolites (Fig. 1), as stated previously.[12]

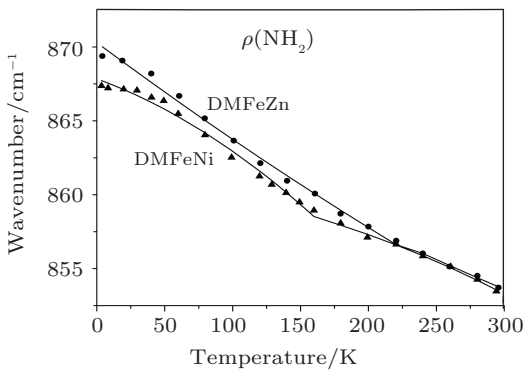

Fig. 1. IR wavenumber of the $\rho(NH_2)$ mode as a function of temperature for DMFeNi and DMFeZn. Solid lines represent Eqs. (6(a))–(6(c)) fitted through Eq. (8) to the observed data.[12]

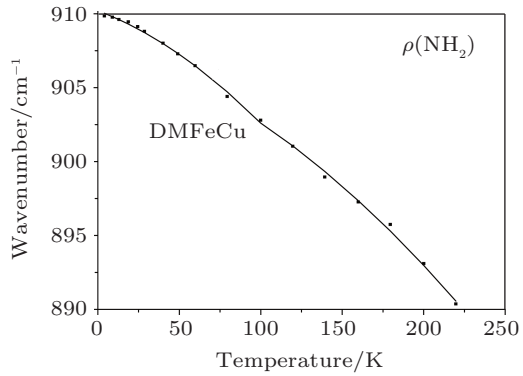

Fig. 2. IR wavenumber of the $\rho(NH_2)$ mode as a function of temperature for DMFeCu. Solid lines represent Eqs. (6(a))–(6(c)) fitted through Eq. (8) to the observed data.[12]

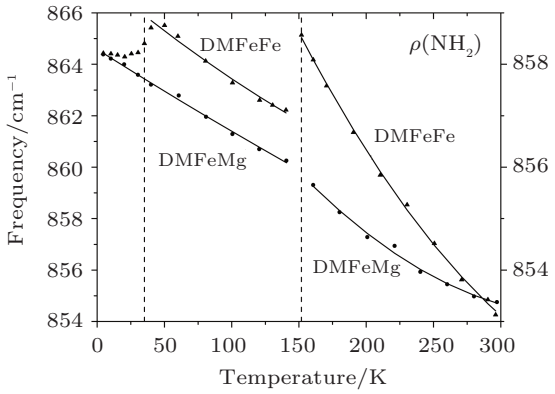

Fig. 3. IR frequency of the $\rho(NH_2)$ mode as a function of temperature for DMFeFe and DMFeMg. Solid lines represent Eqs. (6(a))–(6(c)) fitted through Eq. (8) to the observed data.[13] The vertical lines indicate the temperature where DMFeFe undergoes the structural phase transition.[13]

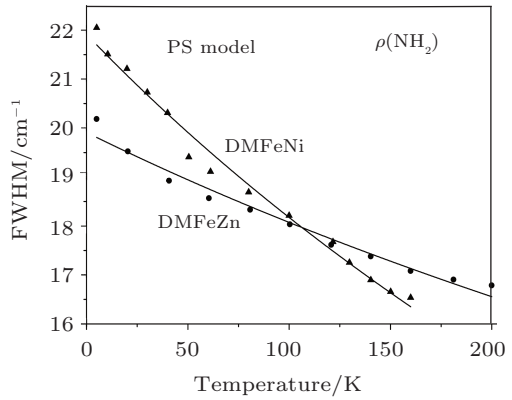

Fig. 4. FWHM of the $\rho(NH_2)$ IR mode as a function of temperature for DMFeNi and DMFeZn below T_c. Solid lines represent Eq. (4) fitted to experimental data[12] according to the pseudospin–phonon coupling model.

The temperature dependence of the damping constant (linewidth) of the $\rho(NH_2)$ internal mode is calculated for those compounds by using the pseudospin–phonon coupling and energy fluctuation models, as plotted in Figs. 4–8. This calculation is performed below T_c with the order parameter S in both models, as stated above. The temperature dependence of the damping constant of the $\rho(NH_2)$ internal mode as predicted from Eqs. (4) (PS model) and (5) (EF model), which are fitted to the observed FWHM,[12] decreases for the trigonal structures (DMFeNi and DMFeZn) (Figs. 4 and 5) whereas it increases for the monoclinic structure (DMFeCu) (Fig. 6) as the temperature increases towards T_c, as also observed experimentally.[12] This indicates that with the intense IR band (shorter FWHM) of the internal $\rho(NH_2)$ mode at low temperatures (well below T_c) for DMFeCu, the monoclinic structures have stronger hydrogen bonds as compared to those of the trigonal structures (DMFeNi and DMFeZn). Above T_c, observed FWHM of the $\rho(NH_2)$ mode tends to increase for DMFeNi and DMFeZn as occurs for the compound DMFeCu with increasing temperature.[12]

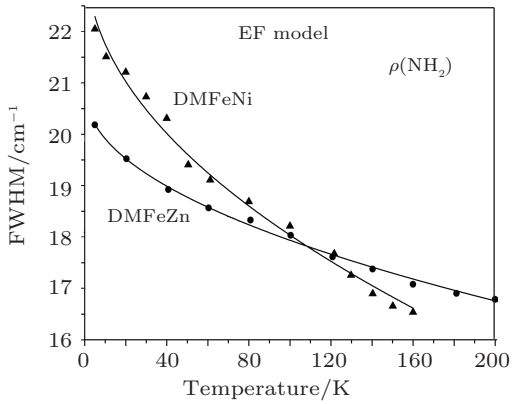

Fig. 5. FWHM of the $\rho(NH_2)$ mode as a function of temperature for DMFeNi and DMFeZn below T_c. Solid lines represent Eq. (5) fitted to experimental data[12] according to the energy fluctuation model.

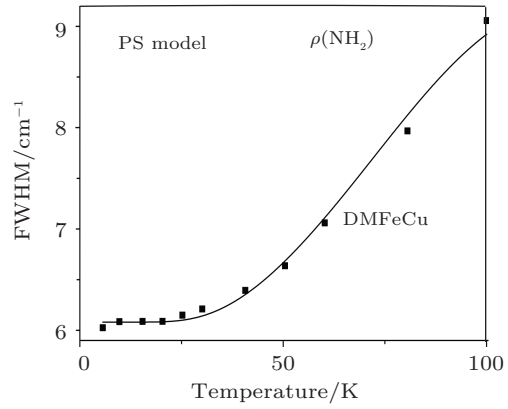

Fig. 6. FWHM of the $\rho(NH_2)$ mode as a function of temperature for DMFeCu. Solid lines represent Eq. (4) fitted to experimental data[12] according to the pseudospin–phonon coupling model.

The abrupt changes in the frequency (Fig. 3) and in particular, in the FWHM (Figs. 7 and 8) of the $\rho(NH_2)$ IR mode show the structural phase transition ($T_c = 151.8$ K) in DMFeFe.[13] This order–disorder phase transition in DMFeFe is due to the freezing-in of reorientational motions of DMA^+ cations which do not lead to any structural phase transition in DMFeMg although at room temperature they show very similar spectra.[13] It has been pointed out that narrowing of bands is much more pronounced for DMFeFe than DMFeMg (Figs. 7 and 8) due to ordering of the DMA^+ cations in DMFeFe at low temperatures and disorder of those cations in DMFeMg down to 4 K.[13] Also, discontinuous changes in frequency or changes in the slope of frequency as a function of

temperature characterize the first-order transition in DMFeFe (Fig. 3).[13] On the other hand, the IR frequencies (Fig. 3) and the FWHM (Figs. 7 and 8) of the $\rho(NH_2)$ mode in DMFeMg do not change abruptly. This indicates that the DMA^+ cations are disordered at low temperatures in DMFeMg, as also pointed out previously.[13] Not only DMFeMg, but also DMFeMn and DMFeCo compounds do not exhibit structural phase transition.[23] This is the main difference between niccolites and DMM (M = Mg, Zn, Mn, Co, Fe, and Ni) perovskites which all exhibit order–disorder phase transitions.[24–29] Due to the $\rho(NH_2)$ IR mode frequencies, a significantly weaker H-bond strength occurs in the niccolate type framework when compared to the perovskite type framework.[13] In the case of DMFeFe niccolite, the $\rho(NH_2)$ IR mode shifts to a lower frequency at T_c, indicating a slight decrease of the hydrogen's bond strength at T_c.[13]

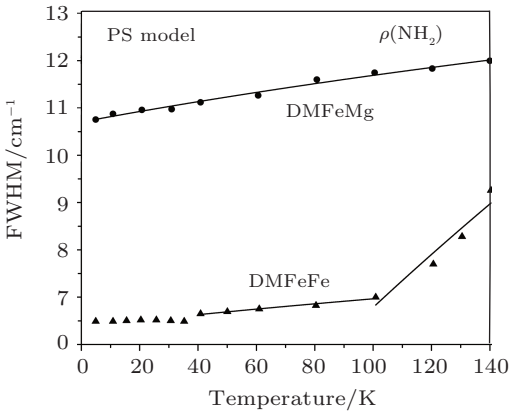

Fig. 7. FWHM of the $\rho(NH_2)$ mode as a function of temperature for DMFeFe and DMFeMg. Solid lines represent Eq. (4) fitted to experimental data[13] according to the pseudospin–phonon coupling model. T_C=151.8 K is the temperature of the structural phase transition in DMFeFe.

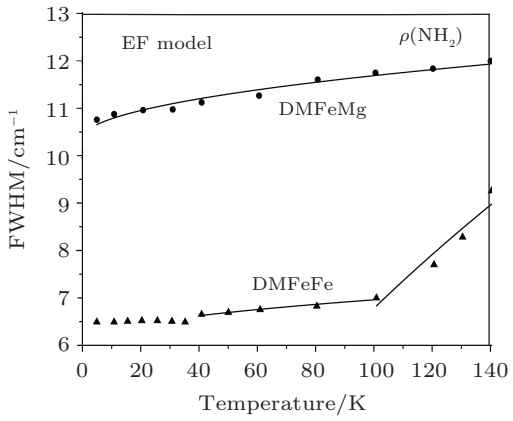

Fig. 8. FWHM of the $\rho(NH_2)$ mode as a function of temperature for DMFeFe and DMFeMg. Solid lines represent Eq. (8) fitted to experimental data[13] according to the energy fluctuation model. T_c = 151.8 K is the temperature of the structural phase transition in DMFeFe.

Our results for the damping constant of the $\rho(NH_2)$ IR mode of the compounds studied (Figs. 4–8) suggest that both models (pseudospin–phonon coupled model and the energy fluctuation model) describe adequately the observed behavior of the FWHM of the internal mode studied, which can be associated with the order parameter in those compounds. Additionally, some other internal modes and also translational and librational modes appearing due to freezing-in of molecular motions and also ordering of DMA^+ cations can be studied by the method given here for the $\rho(NH_2)$ mode. Their frequencies (wavenumbers) can be calculated by the molecular field theory and also their damping constant can be predicted from the pseudospin–phonon coupled and the energy fluctuation models in those MOFs. Regarding the phase transitions in $(CH_3)_2NH_2-Na_{0.5}Fe_{0.5}(HCOO)_3$, namely, DMNaFe as a perovskite, the driving force was stated as the cooperative freezing of the molecular rotation of the DMA^+ cations via hydrogen bonding rather than tilting of the MO_6 octahedra and displacement of the DMA^+ cations.[30] In the family of perovskite heterometallic, $(CH_3)_2NH_2-Na_{0.5}Fe_{0.5}(HCOO)_3$ which exhibits structural phase transition[30] due to ordering of DMA^+ cations,[4,24,30,31] can also be studied by the model, namely, molecular field theory to calculate the order parameter and, the PS and EF models to predict the damping constant as a function of temperature. For this calculation, Raman and IR spectra of modes responsible for the structural phase transition can be analyzed and their wavenumber (order parameter) and FWHM (damping constant) can be predicted by the models studied. It was also stated that this cooperative freezing was shown to be responsible for the onset of a long-range polarization order in DMNaFe.[20] As the temperature decreases, ordering of DMA^+ cations due to freezing of their orientational motions also occurs in the family of compounds with the general formula $(CH_3)_2NH_2M(HCOO)_3$ where M = Mn, Ni, Co, Fe, and Cu,[24,26,32] in particular, DMMg.[33] This freezing leads to strong decrease in FWHM of the $\rho(NH_2)$ band in DMMg and DMCd.[33] Also, the molecular field theory to predict the order parameter (frequency) and to predict the damping constant (FWHM) by the PS and EF models can be applied to some other niccolites and perovskites which exhibit phase transitions.

In fact, very recently, we worked on temperature-induced structural phase transition in $(CH_3)_2NH_2M^{II}(HCOO)_3$, M = Mn, Zn, Fe, Ni, and Mg in the case of M = Mg, shortly DMMg compound, and we calculated the frequency and the linewidth of the ν_s(CNC) and $\rho(NH_2)$ modes[34] by using the experimental data.[35] For the calculation of the frequency, we used the molecular field theory (Eqs. (6a)–(6c)) and for the linewidth (FWHM) the two models (PS and EF) were used, which explained the observed behavior of the wavenumber and FWHM for those IR modes in DMMg. We were not able to analyze the ν_s(CNC) and $\rho(NH_2)$ modes appearing as a function of temperature in $(CH_3)_2NH_2M^{II}(HCOO)_3$, M = Cd or shortly DMCd as observed experimentally[35] by using the same models since this compound does not ex-

hibit any phase transition. However, it shows pressure induced phase transition.[36] We also studied the compounds $NH_4Zn(HCOO)_3$ and deuterium $ND_4Zn(DCOO)_3$ to calculate the IR frequency of the $\nu_4(NH_3^+)$ mode by the molecular field theory and its damping constant (FWHM) by the PS and EF models. We found that for this IR mode, molecular field theory and the PS model work reasonably well whereas EF model does not agree with the experimental data.[37] This can be due to the temperature dependence of the damping constant given by $\Gamma_{sp}\alpha(T-T_c)^{-1/2}$, for example when S=0 ($T > T_c$) for the EF model (Eq. (5)), which holds mostly likely close the phase transition in those compounds. Models were applied to one of the four perovskite type MOFs of $(CH_3NH_2NH_2)M(HCOO)_3$ known as MH_yM, M = Mn, Mg, Fe, and Zn, in particular, MH_yMn which exhibits two structural phase transitions due to partial ordering of the methylhydrazinium (MH_y^+) cations and distortion of the metal organic frameworks.[11] We analyzed the temperature dependence of the wavenumber and the FWHM for the Raman modes of $\nu(NH_2)$, $\nu_s(CH_3)$, $\nu_1(HCOO^-)$, ν_s(CNN), and IR mode of $\rho(NH_2)$ close to the transition temperature ($T_c = 218$ K) in H_yMn by using the experimental data.[11] The models were able to explain the observed behavior of the wavenumber and FWHM for the Raman and IR modes studied in MH_yMn. Since there is a close similarity of MH_yFe to multiferroic $(CH_3)_2NH_2Fe(HCOO)_3$, those models studied (molecular field theory, PS and EF models) can also be applied to those perovskites when the spectroscopic data are available. Similarly, multiferroic perovskites with the general structure of $NH_2NH_3M(HCOO)_3$, M = Mn, Fe, and Zn (H_yM) which exhibit phase transitions, can be studied by using the models employed here. Raman spectra at different temperatures (H_yFe) and at different pressures (H_yZn), which were obtained experimentally,[9] can be analyzed in terms of the wavenumber and FWHM of modes associated with the phase transitions by using the models studied.

As heterometallic niccolites, mixed-valance metal formate with the formulae,

$$(CH_3)_2NH_2Fe^{II}Fe^{III}(HCOO)_6,$$
$$C_2H_5NH_3Fe^{II}Fe^{III}(HCOO)_6,$$
$$(C_2H_5)_2NH_2Fe^{II}Fe^{III}(HCOO)_6,$$

exhibiting multiferroic properties, which undergo structural phase transition ($T_c \approx 240$ K), can also be studied by the models given here although the phase transition is more complex than expected on the basis of an order-disorder model, in particular, for $(CH_3)_2NH_2M(HCOO)_3$ compounds with M = Mn, Zn, Ni, Mg, Fe, and Co, as pointed out previously.[24,25,29,33,38]

4. Conclusions

The IR frequencies of the $\rho(NH_2)$ internal mode were calculated for the DMFeM (M = Ni, Zn, Cu, Fe, and Mg) compounds using the molecular field theory by analyzing the experimental data from the literature. For this calculation, we assumed that the IR frequency of this mode is associated with the order parameter in those structures. We also calculated the damping constant of this mode at various temperatures by using the observed data through the pseudospin–phonon coupled and the energy fluctuation models.

Our results show that the models used for the analysis of the $\rho(NH_2)$ IR mode, are adequate to describe the observed behaviour of the wavenumber and FWHM for niccolite compounds studied. This method of analyzing the frequencies and the linewidth (FWHM) of various modes which are responsible for the phase transitions, can also be applied to some other heterometallic structures.

References

[1] Allendorf M, Bauer C A, Bhakta R K and Houk R J T 2009 *Chem. Soc. Rev.* **38** 1330
[2] Lee J Y, Farha O K, Roberts J, Scheidt K A, Nguyen S B T and Hupp J T 2009 *Chem. Soc. Rev.* **38** 1450
[3] Kreno L E, Leong K, Farha O K, Allendorf M, Duyne R P V and Hupp J T 2012 *Chem. Rev.* **112** 1105
[4] Zhang W and Xiong R G 2012 *Chem. Rev.* **112** 1163
[5] Rogez G, Viart N and Drillon M 2010 *Angew Chem. Int. Ed.* **49** 1921
[6] Mason J A, Veenstra M and Long J R 2014 *Chem. Sci.* **5** 32
[7] Maczka M, Sieradzki A, Bondzior B, Deren P, Hanuza J and Hermanowicz K 2015 *J. Mater. Chem. C* **3** 9337
[8] Ghosh S, Di Sante D and Stroppa A 2015 *J. Phys. Chem. Lett.* **6** 4553
[9] Maczka M, Pasinska K, Ptak M, Paraguassu W, Almeida da Silva T, Sieradzki A and Pikul A 2016 *Phys. Chem. Chem. Phys.* **18** 31653
[10] Clune A J, Hughey K D, Lee C, Abhyankar N, Ding X, Dalal N S, Whangbo M H, Singleton J and Musfeld J L 2017 *Phys. Rev. B* **96** 104424
[11] Maczka M, Gagor A, Ptak M, Paraguassu W, Almeida da Silva T, Sieradzki A and Pikul A 2017 *Chem. Mater.* **29** 2264
[12] Ciupa A, Maczka M, Gagor A, Pikul A and Ptak M 2015 *Dalton Trans.* **44** 13234
[13] Ciupa A, Maczka M, Gagor A, Sieradzki A, Trzmiel J, Pikul A and Ptak M 2015 *Dalton Trans.* **44** 8846
[14] Hagen K S, Naik S G, Huynh B H, Masello A and Christou G J 2009 *Am. Chem. Soc.* **131** 7516
[15] Canadillas-Delgado L, Fabelo O, Rodriguez-Velamazan J A, Lemee-Cailleau M H, Mason S A, Pardo E, Lloret F, Zhao J P, Bu X H, Simonet V, Colin C V and Rodriguez-Carvajal J 2012 *J. Am. Chem. Soc.* **134** 19772
[16] Yamada Y, Mori M and Noda Y 1972 *J. Phys. Soc. Jpn.* **32** 1565
[17] Matsushita M 1967 *J. Chem. Phys.* **65** 23
[18] Lahajnar G, Blinc R and Zumer S 1974 *Phys. Cond. Matter* **18** 301
[19] Schaack G and Winterfeldt V 1977 *Ferroelectrics* **15** 35
[20] Laulicht I 1978 *J. Phys. Chem. Solids* **39** 901
[21] Brout R 1965 *Phase Transitions* (NewYork: Benjamin) pp. 7–44
[22] Yurtseven H and Karacali H 2006 *Spectrochimica Acta A* **65** 421
[23] Zhao J P, Hu B W, Lloret F, Tao J, Yang Q, Zhang X F and Bu X H 2010 *Inorg. Chem.* **49** 10390
[24] Jain P, Ramchandron V, Clark R J, Zhou H D, Toby R H, Dalal N S, Kroto H W and Cheetham A K J 2009 *J. Am. Chem. Soc.* **131** 13625
[25] Fu D W, Zhang W, Cai H L, Zhang Y, Ge J Z, Xiong R G, Huang S D and Nakamura T 2011 *Angew. Chem. Int. Ed.* **50** 11947
[26] Maczka M, Ptak M and Macalik L 2014 *Vib. Spectrosc.* **71** 98

[27] Sanchez-Andujar M, Gomez-Aguirre L C, Pato Doldan B, Yanez-Vilar S, Artiga R, Llamas-Saiz A L, Manna R S, Schnelle S, Lang M, Ritter F, Haghighirad A and Senaris-Rodriguez M A 2014 *Cryst. Eng. Comm.* **6** 3558
[28] Maczka M, Zierkiewicz W, Michalska D and Hanuza J 2014 *Spectrochim. Acta A* **128** 674
[29] Maczka M, Gagor A, Macalik B, Pikul A, Ptak M and Hanuza J 2014 *Inorg. Chem.* **53** 457
[30] Maczka M, Pietraszko A, Macalik L, Sieradzki A, Trzmiel J and Pikul A 2014 *Dalton Trans.* **43** 17075
[31] Shang R, Chen S, Wang Z M and Gao S 2014 *Metal-Organic Framework Materials*, eds. MacGilliuray R L and Lukehart C M (John Wiley Sons) pp. 221–238
[32] Wang W, Yan L Q, Cong J Z, et al. 2013 *Sci. Rep.* **3** 2024
[33] Gou M, Cai H L and Xiong R G 2010 *Inorg. Chem. Commun.* **13** 1590
[34] Yurtseven H and Arslan A 2018 *Ferroelectrics* **526** 9
[35] Szymborska-Malek K, Trzebiatowska-Gutowska M, Maczka M and Gagor A 2016 *Spectrochim. Acta A* **159** 35
[36] Maczka M, Almedia da Silva T, Paraguassu W and Pereira da Silva K 2016 *Spectrochim. Acta. A* **156** 112
[37] Maczka M, Kadlubanski P, Freire P T C, Macalik B, Paraguassu W, Hermanowicz K and Hanuza J 2014 *Inorg. Chem.* **53** 9615
[38] Sanchez-Andujar M, Presedo S, Yanez-Vilar S, et al. 2010 *Inorg. Chem.* **49** 1510